



**Light-induced autoxidation of aldehydes to peracids and  
carboxylic acids**

Journal:	<i>Green Chemistry</i>
Manuscript ID	GC-ART-08-2023-002951.R1
Article Type:	Paper
Date Submitted by the Author:	14-Nov-2023
Complete List of Authors:	Salem, Mohamed; Osaka University, SANKEN; Suez Canal University Faculty of Pharmacy, Pharmaceutical Organic Chemistry Dubois, Carla; Osaka University, SANKEN; Université Paris-Saclay, Département d'Enseignement et de Recherche de Chimie Takamura, Yuya; Shizuoka Institute of Science and Technology, Materials and Life Science Kitajima, Atsuhito; Shizuoka Institute of Science and Technology, Materials and Life Science Kawai, Takuma; Shizuoka Institute of Science and Technology, Materials and Life Science Takizawa, Shinobu; Osaka University, SANKEN Kiriara, Masayuki; Shizuoka Institute of Science and Technology, Materials and Life Science

## ARTICLE

## Light-induced autoxidation of aldehydes to peracids and carboxylic acids

Mohamed S. H. Salem,<sup>a,b</sup> Carla Dubois,<sup>a,c</sup> Yuya Takamura,<sup>d</sup> Atsuhito Kitajima,<sup>d</sup> Takuma Kawai,<sup>d</sup> Shinobu Takizawa\*<sup>a</sup> and Masayuki Kiri-hara\*<sup>d</sup>

Received 00th January 20xx,  
Accepted 00th January 20xx

DOI: 10.1039/x0xx00000x

Autoxidation of aldehydes to peracids and carboxylic acids holds a significant impact in both academia and industry due to their wide applications in organic synthesis and environmental remediation. However, the multiple pathways involved in this reaction have hindered the development of sustainable methods for peracid synthesis. Herein, we conduct a comprehensive kinetic and mechanistic investigation to elucidate the interplay between these pathways. Subsequently, we introduce an efficient eco-friendly method to oxidize aldehydes to their corresponding peracids under sunlight or UV irradiation using oxygen as the sole oxidant without any additives or photocatalysts. Additionally, we demonstrate a simple method for the autoxidation of aldehydes to carboxylic acids *via* controlling key parameters such as the wavelength and solvent. These methods exhibit broad applicability to aromatic and aliphatic aldehydes, successful scaling up to the gram scale, and utilizing renewable solar energy making them good alternatives for traditional methods.

### Introduction

Organic peracids are a widely recognized class of organic compounds with diverse applications in organic synthesis, materials science, and the environmental and medicinal fields.<sup>1</sup> Owing to their distinctive peroxy groups (-O-O-) that readily donate oxygen atoms and compatibility with diverse organic solvents,<sup>2</sup> some organic peracids such as *meta*-chloroperoxybenzoic acid (*m*CPBA) have been considered privileged oxidizing agents for several established reactions (Scheme 1A).<sup>1d</sup> Organic peracids are commonly synthesized by the perhydrolysis of carboxylic acids, acid chlorides, or anhydrides with hydrogen peroxide (H<sub>2</sub>O<sub>2</sub>).<sup>3</sup> Other approaches, such as the photoinduced peroxidation of alkyl arenes (e.g., toluene), have recently been introduced to afford aromatic peracids.<sup>4</sup> Autoxidation of aldehydes to carboxylic acids and peracids is one of the most appealing methods, primarily because of the readily available and cost-effective nature of aldehydes (Scheme 1B).<sup>5</sup> Early reports used superstoichiometric amounts of hazardous oxidants with low atom efficiency, such as permanganate, chromate, perborate, percarbonate, and oxone.<sup>6</sup> To address this problem, various strategies have been

implemented using molecular oxygen as a greener alternative for the oxidation of aldehydes *via* organo-*[N*-hydroxyphthalimide (NHP)]<sup>7</sup> or metal-catalyzed (Cu, Ag, Ni, Mn, Fe, and Pt) approaches.<sup>8</sup> Recently, Wang et al. disclosed an aerobic pH-adjusted method,<sup>9</sup> and He et al. introduced a thermo-induced approach for the oxidation of aldehydes.<sup>10</sup>

The concept of the photoexcitation of aldehydes to form a triplet radical pair, which initiates a radical-mediated pathway towards the corresponding peracids and carboxylic acids, has a long history.<sup>11</sup> Apart from a few early reports that studied the photoinduced ozone-initiated oxidation of benzaldehyde to perbenzoic acid,<sup>12</sup> most recent efforts have been dedicated to investigating the photoinduced oxidation of aldehydes to carboxylic acids.<sup>13</sup> In the pursuit of aldehyde autoxidation, Safari et al. used porphyrin as a photocatalyst under visible light conditions,<sup>13b</sup> Cho et al. applied Ru/Ir-based photocatalysts under blue light,<sup>13c</sup> and Favre-Réguillon et al. used camphorquinone under white light in a flow photochemical system.<sup>13d</sup> Despite recent significant advancements, most of these approaches cannot avoid the use of organo- and metal catalysts, other additives, hazardous solvents, buffers, or strong bases, and many of them require complex setups, high pressures of molecular oxygen, or elevated temperatures, which hinder their classification as green and environmentally friendly processes.

In 2022, three groups independently reported highly atom-efficient and green photoinduced protocols for the aerobic oxidation of aldehydes to their corresponding carboxylic acids (Scheme 1C).<sup>13e-g</sup> Li et al. used molecular oxygen and water as the main solvent to afford carboxylic acids without catalysts or additives.<sup>13e</sup> Hashmi et al. demonstrated a sunlight-induced protocol using air, rather than pure oxygen, and acetone as the solvent.<sup>13f</sup> Kokotos et al. applied two conditions, sunlight, and

<sup>a</sup> SANKEN, Osaka University, Mihogaoka, Ibaraki-shi, Osaka 567-0047, Japan.

E-mail: taki@sanken.osaka-u.ac.jp

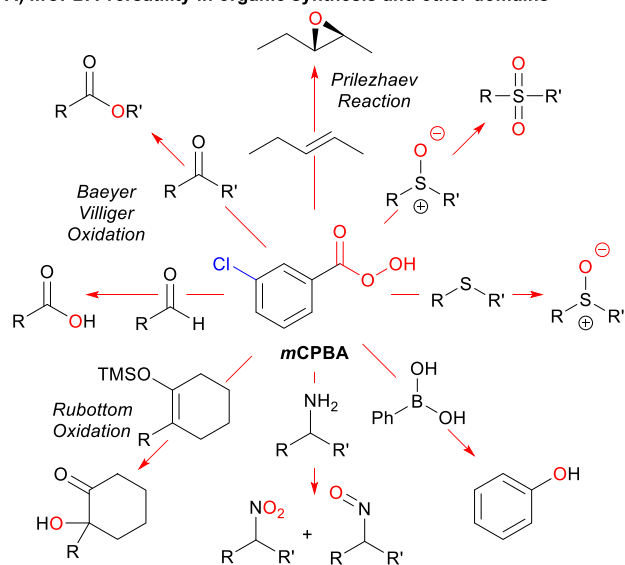
<sup>b</sup> Pharmaceutical Organic Chemistry Department, Faculty of Pharmacy, Suez Canal University, Ismailia 41522, Egypt.

<sup>c</sup> Département d'Enseignement et de Recherche de Chimie, Université Paris-Saclay, ENS Paris-Saclay, 91190 Gif-sur-Yvette, France.

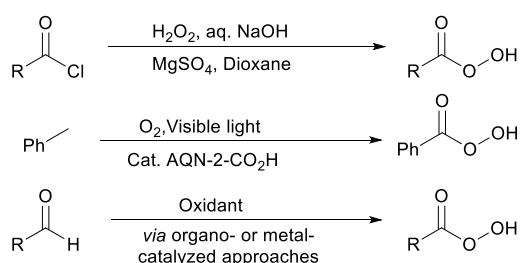
<sup>d</sup> Department of Materials and Life Science, Shizuoka Institute of Science and Technology, 2200-2 Toyosawa, Fukuroi, Shizuoka 437-8555, Japan. E-mail: kiri-hara.masayuki@sist.ac.jp

† Footnotes relating to the title and/or authors should appear here.

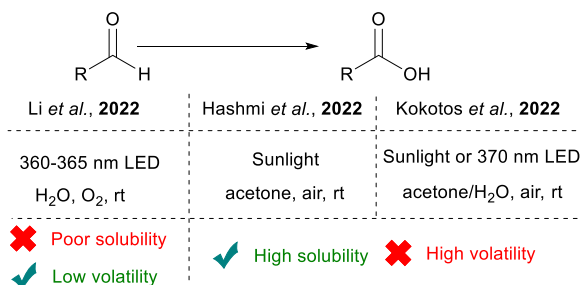
Electronic Supplementary Information (ESI) available: [details of any supplementary information available should be included here]. See DOI: 10.1039/x0xx00000x

A) *m*CPBA versatility in organic synthesis and other domains

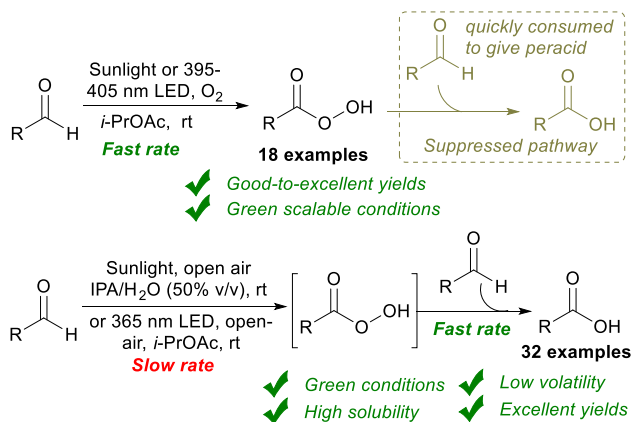
## B) Previous methods



## C) Light-promoted oxidation of aldehydes to carboxylic acids



## D) This work: oxidation of aldehydes to peracids and carboxylic acids



**Scheme 1** Applications and synthetic approaches for peracids: previous methods and this work.

370 nm irradiation, to afford carboxylic acids (Scheme 1C).<sup>13g</sup> However, the photoinduced oxidation of aldehydes to their corresponding organic peracids has been underexplored, and the few explored protocols have either required high concentrations of organocatalysts (NHPI)<sup>14</sup> or encountered challenges such as generalizing their findings or effectively separating the peracids.<sup>13f</sup> These limitations arose mainly from the multiple reaction pathways for the liquid-phase aerobic oxidation of aldehydes and how these pathways interfere with the conversion of peracids to the corresponding carboxylic acids.<sup>15</sup> Herein, we further explore the competition between these interfering reaction pathways through mechanistic and kinetic studies. Building on our understanding and fine-tuning of all the reaction parameters, we established efficient, scalable, and eco-friendly conditions for the oxidation of aldehydes to their corresponding peracids under sunlight and UV irradiation. Varying key parameters (wavelength and solvent) provided alternative efficient conditions for synthesizing the corresponding carboxylic acids using sunlight or UV light (Scheme 1D).

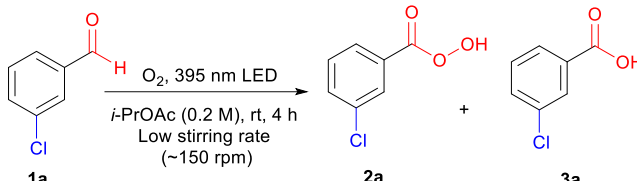
## Results and discussion

### Exploring the reaction and condition optimizations

To investigate the photoinduced autoxidation of aldehydes to the corresponding peracids, *meta*-chlorobenzaldehyde **1a** was chosen as the model starting material because of the favorable properties of *m*CPBA **2a**, ensuring high safety and ease of handling.<sup>14</sup> With *iso*-propyl acetate (*i*-PrOAc) as the solvent and 395 nm irradiation under an oxygen atmosphere for 4 h (see ESI for details), **2a** was obtained in a 79% yield (Table 1, entry 1). Light played a critical role in this reaction, because no product was observed under dark conditions (Table 1, entry 2). Shorter wavelengths (340–365 nm) afforded higher **3a/2a** ratios, whereas longer wavelengths (521–631 nm) resulted in lower conversions (Table 1, entries 3 and 4, and Fig. 1A). Advantageously, sunlight irradiation gave a comparable 72% yield (Table 1, entry 5), which did not occur with indoor light because of its different power and wavelength spectra (Table 1, entry 6). In pursuit of a simpler setup, we replaced pure oxygen with air; however, the yield was reduced because of the activation of the side pathways at the expense of the main pathway (Table 1, entry 7). Under a nitrogen atmosphere, the reaction was suppressed, highlighting the crucial role of oxygen (Table 1, entry 8). Owing to the vulnerability of peracids to mechanical and thermal decomposition,<sup>16</sup> we optimized our conditions at a low stirring rate (< 200 rpm) to avoid any negative physical effects caused by vigorous stirring (see ESI for details), which agrees with the observed lower yields at higher stirring rates (Table 1, entry 9).

Considering the critical role of the solvent,<sup>17</sup> we conducted a comprehensive screening of approximately 24 solvents under 405 nm (see ESI for details), 395 nm, and sunlight irradiation (Fig. 1B and 1C). With alcoholic solvents, lower conversions were observed owing to the suppressed reaction rates, which

could be attributed to the strong intermolecular forces (H-bonding) between these solvents and the aldehydes.<sup>17b</sup> Etheral solvents such as tetrahydrofuran (THF) and 1,4-dioxane afforded only carboxylic acid **3a** in modest yields (< 20%), whereas methyl *tert*-butyl ether (MTBE) provided 42% of **3a** and 4.5% of **2a**, respectively. In contrast, chlorinated solvents afforded significantly higher yields of carboxylic acid **3a** (>95%) than those achieved with other solvents, primarily because of their higher rates. However, dichloroethane (DCE) yielded a mixture of **3a** and **2a** in a 2:1 ratio. Some nonpolar solvents (toluene and cyclohexane) and polar aprotic solvents [dimethylsulfoxide (DMSO) and dimethylformamide (DMF)] displayed low conversion rates, yielding only carboxylic acid **3a** as the over-oxidation product. The use of water or neat conditions led to high yields of carboxylic acid **3a** with no observation of peracid **2a**. Some solvents showed promising results for the formation of **2a**, such as acetone (31%) and acetonitrile (51%), while the best results were achieved with ester solvents [ethyl acetate (EtOAc), 62% and *i*-PrOAc, 72%]. In recent years, *i*-PrOAc has demonstrated significant value across numerous industrial and academic applications as a green and cost-efficient solvent,<sup>18</sup> with some early studies highlighting its advantage in decreasing the decomposition rate of benzoyl peroxide.<sup>19</sup>

**Table 1** Screening of reaction conditions


Entry	Variation from standard conditions	2a (%)	3a (%)
1	None	79	20
2	No light	-	trace
3	365 nm LED	28	68
4	521 nm LED	-	27
5	Outdoor sunlight	72	21
6	Indoor artificial light	-	44
7	Open air	54	45
8	Under nitrogen	-	trace
9	Stirring rate = 400 rpm	68	30
10	Ethanol (0.2 M)	-	21

Reaction conditions: **1a** (0.25 mmol), *i*-PrOAc (1.25 mL), under oxygen atmosphere at room temperature. Yields were determined by <sup>1</sup>H-NMR.

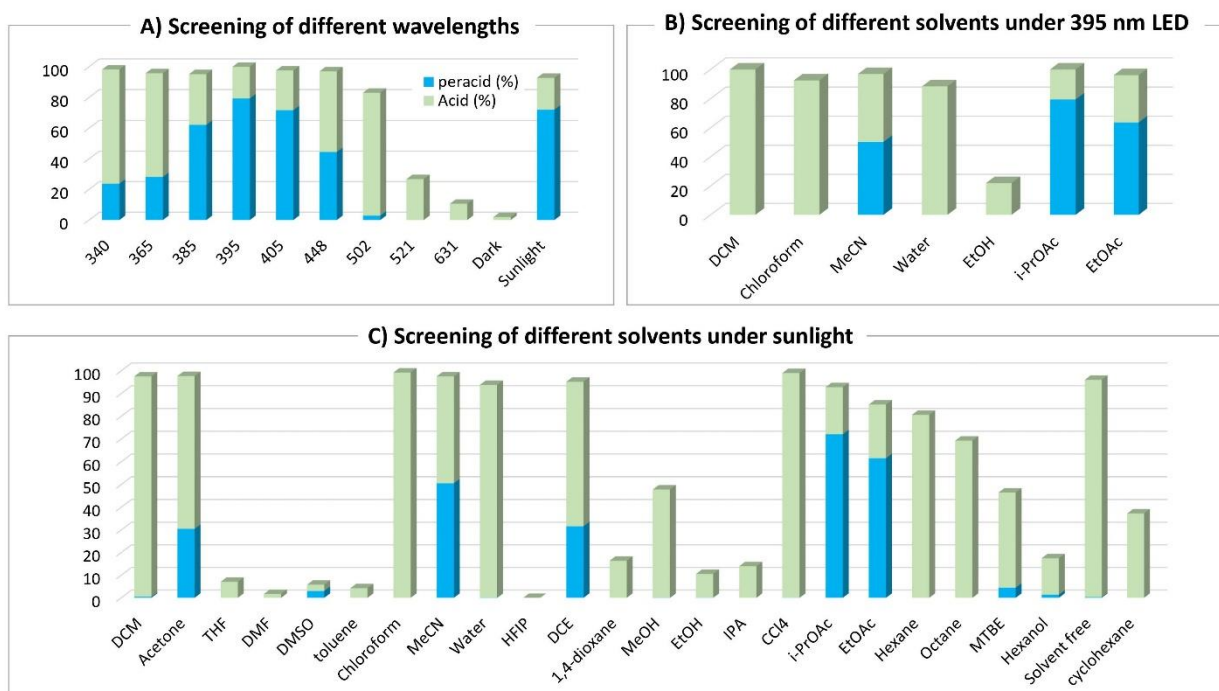


**Fig. 1** Effect of different wavelengths and solvents on the reaction progress and peracid **2a**/carboxylic acid **3a** ratio. Reaction conditions: **1a** (0.25 mmol), solvent (1.25 mL), under an oxygen atmosphere at room temperature (stirring rate = 150 rpm) for 4 h.

### Mechanistic and kinetic investigations

To gain deeper insight into the critical role of solvents in suppressing or encouraging interfering reaction pathways, we conducted a detailed kinetic analysis under various conditions (see ESI for details). Autoxidation of aldehydes begins with photoexcitation and reaction with oxygen through a radical-

mediated pathway, generating the corresponding peracid **2a** at rate  $k_a$  (Fig. 2A). Following a mechanism similar to Baeyer-Villiger oxidation,<sup>20</sup> the corresponding carboxylic acid **3a** can be formed *via* a Criegee intermediate at rate  $k_b$ . Another pathway for the rearrangement of the Criegee intermediate has been reported,<sup>17, 21</sup> which can afford a mixture of formate **4a** and

carboxylic acid **3a**. Luckily, formate byproduct **4a** was not observed under our conditions for substrate **1a**.<sup>17a</sup> Additionally, carboxylic acid **3a** was formed by the direct decomposition of **2a** at rate  $k_c$ .<sup>14</sup> Favre-Réguillon et al. investigated these pathways and the key factors that favored one pathway over another.<sup>14, 21-22</sup> Lehtinen et al. and Jin, Peng, Zhao et al. have demonstrated the effect of the solvent on the rearrangement of peracid-aldehyde adducts during the aerobic autoxidation of aldehydes *via* experimental and computational efforts.<sup>17</sup> However, most of these mechanistic investigations have focused on the competition between the two pathways governing the rearrangement of the Criegee intermediate ( $k_b$  vs.  $k_d$ ) and used an aliphatic aldehyde (2-ethylhexanal) to conduct their investigation. Herein, our primary focus is to analyze the interplay between the pathways involved in the production of the peracid and its subsequent degradation ( $k_a$  vs.  $k_b$  and  $k_c$ ) to determine the optimal conditions for peracid synthesis and to ascertain the most suitable point to terminate the reaction. Our system can be defined using three ordinary differential equations (ODEs) as follows:

$$\frac{d[1a]}{dt} = -k_a[1a] - k_b[1a][2a] \quad (1)$$

$$\frac{d[2a]}{dt} = k_a[1a] - k_c[2a] - k_b[1a][2a] \quad (2)$$

$$\frac{d[3a]}{dt} = k_c[2a] + 2 k_b[1a][2a] \quad (3)$$

Tracking the changes in the concentrations of **1a**, **2a**, and **3a** as a function of time under different initial conditions (Fig. 2B) enabled the calculation of  $k_a$ ,  $k_b$ , and  $k_c$  values through nonlinear regression analysis (*via* Python's SciPy library) and fitting our experimental data to the ODEs (Eq. 1-3) (see ESI for details). By solving these equations, we modeled the concentration profiles of each species over time to visualize their generation and consumption under different conditions (Fig. 2C). Kinetic analysis revealed that the direct decomposition of **2a** into **3a** occurred at an extremely low rate compared to the other pathways, suggesting a negligible effect, especially with shorter reaction times. The primary competing pathways involved the generation of **2a** from **1a** and the subsequent reaction of **1a** and **2a** producing **3a**. Under sunlight irradiation with *i*-PrOAc as the solvent, the rate constant ( $k_b = 0.05215 \text{ min}^{-1}$ ) for the reaction between **1a** and **2a** was 1.67 times faster than the rate constant ( $k_a = 0.03119 \text{ min}^{-1}$ ) for the generation of **2a**; however, the significance of this side reaction ( $k_b$ ) depends on the concentrations of both **1a** and **2a**. Owing to the fast conversion of **1a** to **2a** under these conditions, the time frame when both concentrations of **1a** and **2a** are relatively high is very short, minimizing the effect of this side pathway (Fig. 2C-I). In contrast, other solvents such as methanol- $d_4$  showed a  $k_b$  rate approximately 400 times faster than  $k_a$ , which explains why peracid **2a** was not observed during the time-course study. The reason for the low conversion of **1a** to **3a** in methanol- $d_4$  (Fig. 1C), despite the smooth progression of the reaction between **1a** and **2a** to form **3a**, can be attributed to the slow rate-limiting step of **1a** to **2a** conversion (Fig. 2C-II). The kinetic study was extended to other light sources and wavelengths (see ESI for details).

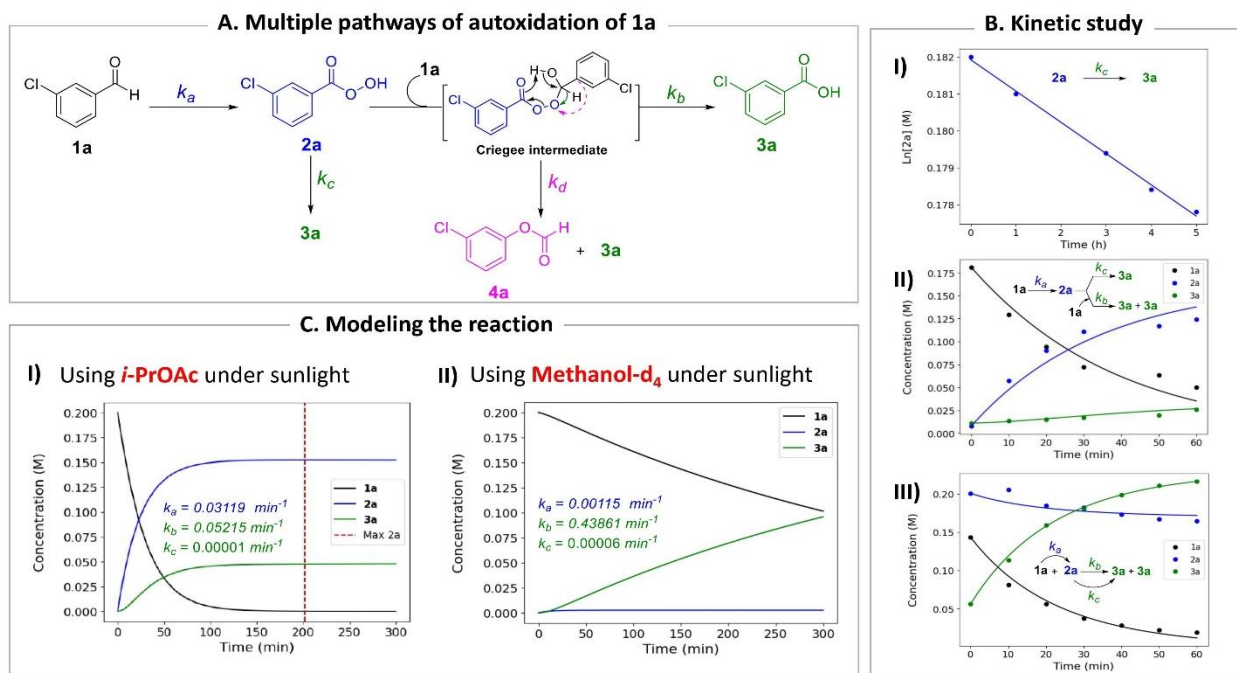
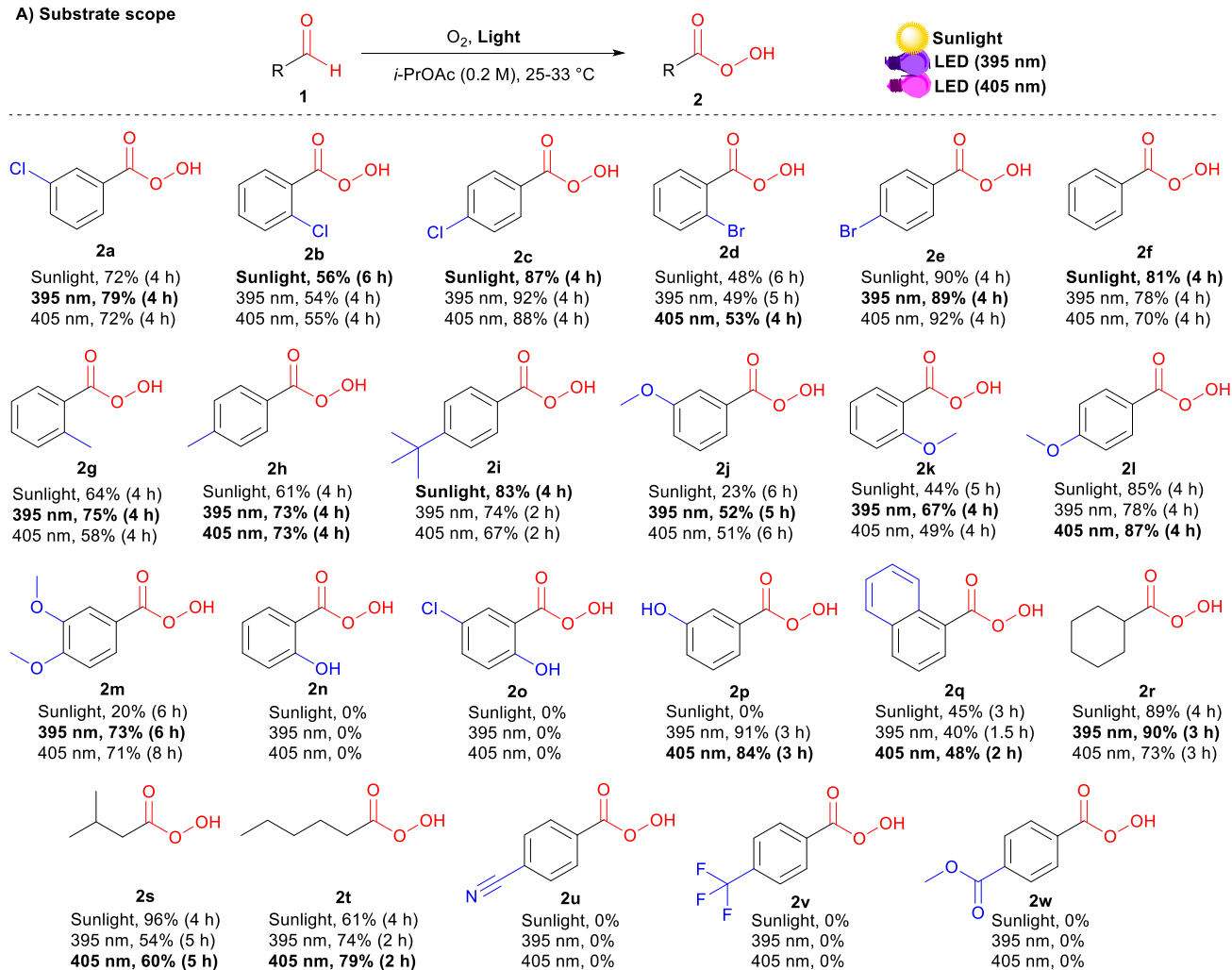
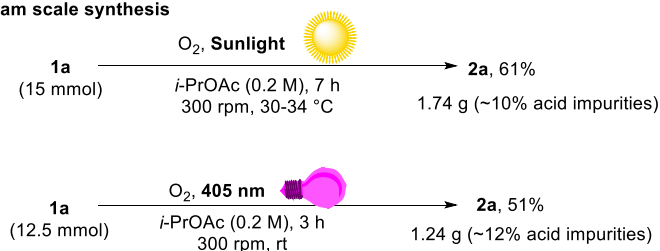


**Fig. 2** Kinetic study. **A**) Multiple pathways for the autoxidation of *meta*-chlorobenzaldehyde (**1a**). **B**) Kinetic analysis: (I) calculation of the rate of peracid decomposition  $k_c$ ; (II) and (III) calculation of the rates  $k_a$  and  $k_b$ . **C**) Modeling the autoxidation of aldehyde **1a** under different conditions: (I) using *i*-PrOAc as a solvent under sunlight and (II) using MeOH- $d_4$  as a solvent under sunlight.

## A) Substrate scope



## B) Gram scale synthesis

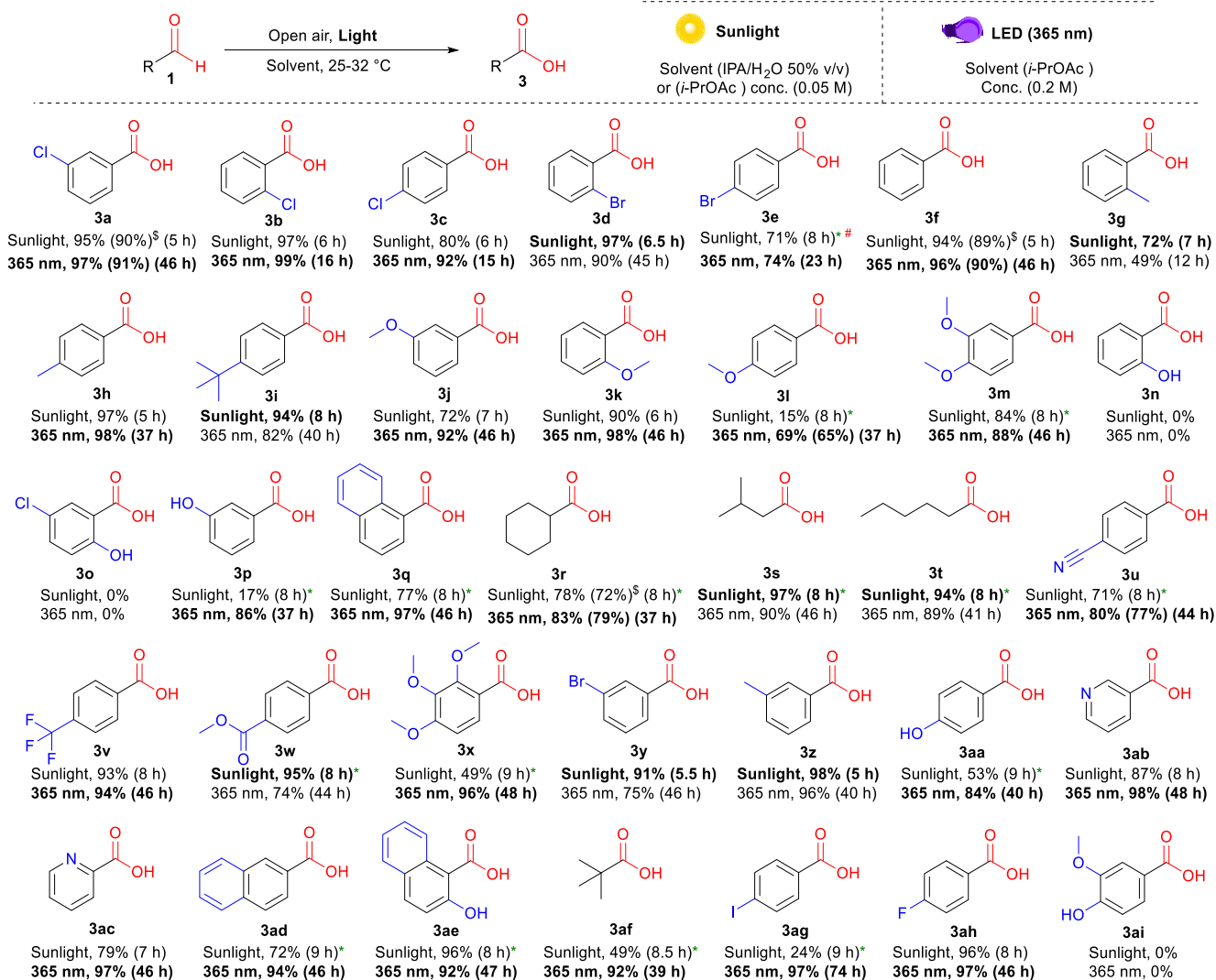


**Scheme 2** Substrate scope and scalability for the photoinduced oxidation of aldehydes to peracids. **A)** Reaction conditions **1** (0.25 mmol), *i*-PrOAc (1.25 mL), under an oxygen atmosphere (stirring rate = 150 rpm) at 25–33 °C. The yields were determined by <sup>1</sup>H-NMR. Bold conditions are recommended for a good balance between high yield and safety (keeping the purity ~70–75%, with ~10% carboxylic acid impurities, is favourable in terms of stability and safety). **B)** Gram scale synthesis of *m*CPBA under sunlight and 405 nm LED irradiation: reaction conditions **1a** (12.5–15 mmol), *i*-PrOAc (0.2 M), under an oxygen atmosphere (stirring rate = 300 rpm) at 25–34 °C. The isolated yields are reported.

## Exploring the scope of peracids

With the three high-yielding conditions in hand (see ESI for details), the substrate scope of peracid **2** was investigated (Scheme 2A). Generally, unsubstituted (**2f**) and *para*-substituted aromatic aldehydes bearing electron-donating (EDGs; **2h**, **2i**, and **2l**) or halogens (**2c** and **2e**) afforded higher yields than their *ortho*- and *meta*-substituted analogs (**2a**, **2b**, **2d**, **2g**, **2j**, and **2k**). This result

highlights how both electronic and steric effects play key roles in the reactivities of different substrates in the multiple pathways. Accordingly, some substrates required either shorter or longer reaction times to obtain the maximum possible peracid yield. Dimethoxy-substituted benzaldehyde afforded good yields under LED irradiation (395 and 405 nm), whereas lower yields were observed under sunlight owing to the slower reaction rate (**2m**).



**Scheme 3** Substrate scope for the photoinduced oxidation of aldehydes to carboxylic acids. Reaction conditions (under sunlight): **1** (0.0625 mmol), IPA/water 50% v/v (1.25 mL), under open air (stirring rate = 500 rpm) at 25–32 °C. The yields were determined by <sup>1</sup>H-NMR (isolated yields in parentheses). # (conc. = 0.025 M). \* (solvent = *i*-PrOAc). <sup>§</sup> (0.25 mmol scale). Reaction conditions (under 365 nm LED): **1** (0.25 mmol), *i*-PrOAc (1.25 mL), open air (stirring rate = 500 rpm) at room temperature. The yields were determined by <sup>1</sup>H-NMR (isolated yields in parentheses).

Stable *ortho*-substituted hydroxybenzaldehydes were resistant to photoinduced oxidation under additive-free conditions (**2n** and **2o**),<sup>23</sup> while their *meta*-substituted analogs (**2p**) afforded high yields of 91% and 84% under 395 nm and 405 nm irradiation, respectively. Aliphatic aldehydes were highly compatible with our conditions, giving the corresponding peracids in good yields (**2r–2t**). Benzaldehydes bearing electron-withdrawing groups (EWGs) showed very slow reaction rates, which terminated the possibility of peracid accumulation, as all generated peracids were directly converted to their corresponding carboxylic acids at a faster rate (**3u–2w**). Then, a gram scale synthesis was performed to give approximately 1.74 g (90% peracid) and 1.24 g (88% peracid) of **2a** under sunlight and 405 nm irradiation, respectively (Scheme 2B).

### Exploring the scope of carboxylic acids

After the details of the reaction mechanism were clarified through our kinetic studies, further green and efficient methods for converting the peracids produced *in situ* into carboxylic acids were also explored. Based on our understanding of the role of different wavelengths and solvents in activating and suppressing competing pathways, we further optimized alternative conditions using a different wavelength (365 nm LED) or solvent system [*iso*-propyl alcohol (IPA)/water, 50% v/v] for the production of carboxylic acids **3** from aldehydes **1** using air as a safer and cheaper alternative to pure oxygen. We employed a mixed solvent system under sunlight irradiation to effectively address the most controversial aspects encountered in prior works<sup>13e-g</sup> concerning solubility and volatility.<sup>24</sup> A broad spectrum of aliphatic and aromatic aldehydes with various

EWGs and EDGs at different positions afforded carboxylic acids in high yields under the optimized conditions (Scheme 3). Some aldehydes displayed slower reaction rates ( $k_a$ ) in water-containing mixed solvent systems under sunlight. Hence, we utilized *i*-PrOAc as an alternative solvent, taking advantage of their slower ( $k_a$ ) rates, which would prevent the unwanted accumulation of peracids during the reaction (**3l**, **3m**, **3p–3u**, **3w**, **3x**, **3aa**, and **3ad–3ag**). Multi-methoxy-substituted benzaldehydes (**3m** and **3x**), heterocyclic aldehydes (**3ab** and **3ac**), and naphthaldehydes (**3q**, **3ad**, and **3ae**) gave good yields, especially under 365 nm irradiation. Although *para*-fluoro- (**3ah**) and *para*-chlorobenzaldehydes (**3c**) exhibited excellent yields under sunlight, their bromo- (**3e**) and iodo- (**3ag**) counterparts were less efficient under these conditions. Even with high dilution and scaling down, the yield of **3e** could not be enhanced beyond 71%; however, all these substrates showed excellent yields when irradiated at 365 nm for longer times. Similar to peracids, *ortho*-substituted hydroxybenzaldehydes (**3n** and **3o**) and vanillin (**3ai**) resisted photoinduced oxidation under additive-free conditions.

### Control experiments

To further support the aldehyde autoxidation mechanism, some control experiments were performed. Light on/off experiments revealed the indispensability of continuous irradiation for the generation of peracid **2a** from aldehyde **1a** (Fig. 3). In the absence of light, the primary pathway leading from **1a** to **2a** was entirely suppressed, whereas the secondary pathway involving the Baeyer-Villiger rearrangement remained partially active, demonstrating the partial consumption of **2a** and the concurrent generation of **3a**.

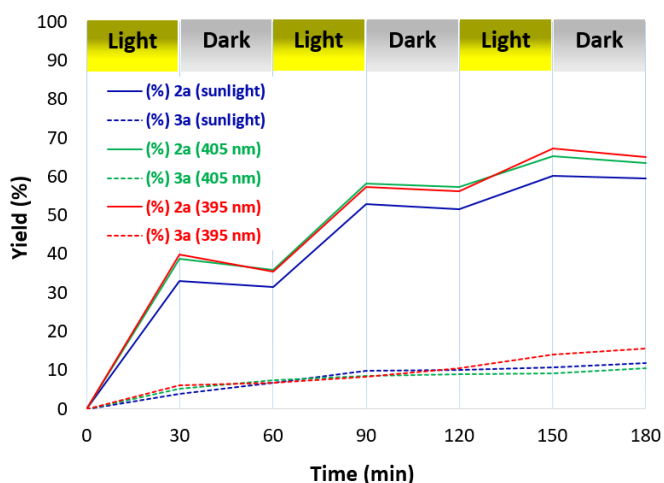
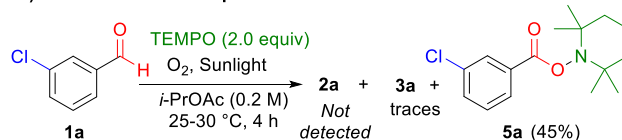


Figure 3 Light-irradiation on/off experiments

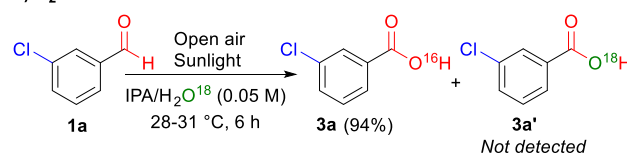
In the presence of the radical scavenger tetramethylpiperidine-1-oxyl (TEMPO), both carboxylic acid **3a** and peracid **2a** were not observed, which is consistent with the accepted radical-mediated pathway (Scheme 4A). When  $^{18}\text{O}$ -isotope labeled water was used in place of water under the optimized conditions for carboxylic acids, no  $^{18}\text{O}$ -labeled carboxylic acid **3a'** was observed, confirming that the origin of the oxygen atom in the product was the oxygen atmosphere rather than water (Scheme 4B). A plausible mechanism (Scheme 4C) can be proposed based on our control experiments (Fig. 3 and

Scheme 4), kinetic analysis (Fig. 2), and related reports.<sup>11e, 13e-g, 21, 22b</sup> Under light irradiation, aldehyde **1** is excited to form a highly reactive triplet radical pair (**I** and **II**), which undergoes a radical-mediated pathway with molecular oxygen to generate the corresponding peroxy radicals (**III** and **IV**). Peroxy radical **III** subsequently engages in a hydrogen atom transfer (HAT) reaction to form peracid **2** and benzoyl radical **I**. Through a pathway similar to Baeyer-Villiger oxidation,<sup>20</sup> the corresponding carboxylic acid **3** can be formed *via* a Criegee intermediate. This intermediate is produced by the nucleophilic addition of peracid **2** or radical **IV** to aldehyde **1**.

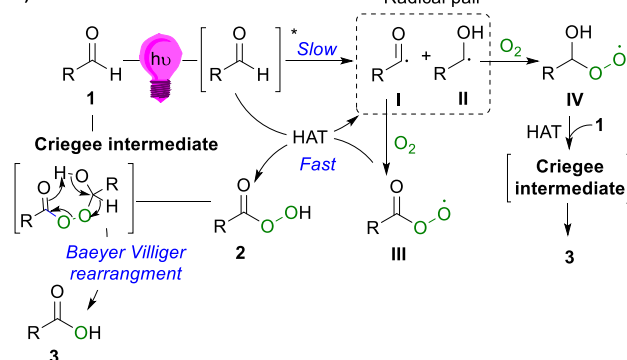
### A) Radical inhibition experiment



### B) $\text{H}_2\text{O}^{18}$ instead of water



### C) Plausible mechanism



Scheme 4 Control experiments and plausible mechanism.

## Conclusions

To explore the liquid-phase autoxidation of aldehydes, we conducted detailed kinetic and mechanistic studies to elucidate the key factors affecting the different rates of each step. We then developed an eco-friendly, practical, and simple photoinduction method to afford peracids in high-to-excellent yields using oxygen as the sole oxidant under sunlight or UV light irradiation. The substrate scope and limitations were carefully examined, and the scalability of this protocol was validated. An alternative green and efficient method for the production of various carboxylic acids in open air was introduced after adjusting the wavelength and solvent system. Further investigations for the nature of interactions between the solvents and reaction intermediates is currently under progress.

## Experimental section

### Gram-scale synthesis of mCPBA 2a

To a dry 100 mL two-neck round-bottom flask, *meta*-chlorobenzaldehyde (**1a**, 15 mmol) and *i*-PrOAc (60 mL) were added under an oxygen atmosphere (using the Schlenk line). The mixture was stirred (using a 20 mm magnet at 300 rpm) under sunlight at 30–34 °C. The progress of the reaction was monitored by No-D <sup>1</sup>H-NMR spectroscopy. After 7 h, the reaction was stopped after reaching a plateau, and the solution was directly concentrated *in vacuo* (avoiding heating or high-speed rotation during concentration). The obtained compounds were washed with phosphate buffer (pH = 7.2 × 25 mL), extracted with ethyl acetate, dried over anhydrous sodium sulfate, and evaporated to obtain the final mCPBA **2a** (1.74 g) containing approximately 10% acid impurities. Further purification was avoided, primarily because of safety concerns. Pure peracids are highly shock-sensitive and may explode or decompose under thermal or mechanical stress. Maintaining approximately 10% acid impurities in the sample is advisable, which aligns with commercially available mCPBA, ensuring both a reasonable level of purity and high yields.

**Additional reaction information:** place: (Osaka, Japan); date (04/07/2023); weather (sunny); outdoor temperature (30–34 °C); time (11:00 am–18:00 pm); humidity (41–48%); wind (3.2–14.5 km/h).

### Author Contributions

M. S. H. S.: Designing the experiments, writing the paper, performing experiments and analysing the data. C. D., Y. T., A. K., and T. K.: Performing experiments and analysing the data. S. T. and M. K.: Supervising the project and editing the final version of the manuscript.

### Conflicts of interest

There are no conflicts to declare.

### Acknowledgements

We thank Prof. Makoto Yasuda and Dr. Yoshihiro Nishimoto for generously affording us high-power LED light for the large-scale synthesis. We are very appreciative to Amr Shaalan and Rashed Almasri for their insightful discussions and support during conducting the kinetic study. We also acknowledge the technical staff of the Comprehensive Analysis Center of SANKEN, Osaka University (Japan). The computational part was performed at the Research Center for Computational Science, Okazaki (IMS-RCCS-A-ja). This work was supported by JSPS KAKENHI Grant Numbers 21A204, 21H05217 and 22K06502, 21A204 from the Ministry of Education, Culture, Sports, Science, and Technology (MEXT), the Japan Society for the Promotion of Science (JSPS), JST CREST (No. JPMJCR20R1), and Hoansha Foundation.

## Notes and references

- (a) D. Kiejza, U. Kotowska, W. Polińska and J. Karpińska, *Sci. Total Environ.*, 2021, **790**, 148195; (b) C. Shi, C. Li, Y. Wang, J. Guo, S. Barry, Y. Zhang and N. Marmier, *Water*, 2022, **14**, 2309; (c) N. Kaur and D. Kishore, *Synth. Commun.*, 2014, **44**, 721; (d) H. Hussain, A. Al-Harrasi, I. R. Green, I. Ahmed, G. Abbas and N. U. Rehman, *RSC Adv.*, 2014, **4**, 12882; (e) Y. Zhu, Q. Wang, R. G. Cornwall and Y. Shi, *Chem. Rev.*, 2014, **114**, 8199; (f) T. Luukkonen and S. O. Pehkonen, *Crit. Rev. Env. Sci. Technol.*, 2017, **47**, 1.
- D. Swern, *Chem. Rev.*, 1949, **45**, 1.
- (a) B. T. Brooks and W. B. Brooks, *J. Am. Chem. Soc.*, 1933, **55**, 4309; (b) L. S. Silbert, E. Siegel and D. Swern, *J. Org. Chem.*, 1962, **27**, 1336; (c) J. Moyer and N. Manley, *J. Org. Chem.*, 1964, **29**, 2099; (d) Y. Ogata and Y. Sawaki, *Tetrahedron*, 1967, **23**, 3327.
- M. Taguchi, Y. Nagasawa, E. Yamaguchi, N. Tada, T. Miura and A. Itoh, *Tetrahedron Lett.*, 2016, **57**, 230.
- (a) S. Caron, R. W. Dugger, S. G. Ruggeri, J. A. Ragan and D. H. B. Ripin, *Chem. Rev.*, 2006, **106**, 2943; (b) J.-E. Bäckvall, *Modern oxidation methods*, John Wiley & Sons, 2011.
- (a) B. Ganem, R. P. Heggs, A. J. Biloski and D. R. Schwartz, *Tetrahedron Lett.*, 1980, **21**, 685; (b) B. S. Bal, W. E. Childers Jr and H. W. Pinnick, *Tetrahedron*, 1981, **37**, 2091; (c) S. O. Nwaukwa and P. M. Keehn, *Tetrahedron Lett.*, 1982, **23**, 3131; (d) A. McKillop and D. Kemp, *Tetrahedron*, 1989, **45**, 3299; (e) A. McKillop and W. R. Sanderson, *Tetrahedron*, 1995, **51**, 6145; (f) B. R. Travis, M. Sivakumar, G. O. Hollist and B. Borhan, *Org. Lett.*, 2003, **5**, 1031; (g) M. Hunsen, *Synthesis*, 2005, **2005**, 2487; (h) R. Bernini, A. Coratti, G. Provenzano, G. Fabrizi and D. Tofani, *Tetrahedron*, 2005, **61**, 1821; (i) M. Shibuya, T. Sato, M. Tomizawa and Y. Iwabuchi, *Chem. Commun.*, 2009, **2009**, 1739; (j) J. Sedelmeier, S. V. Ley, I. R. Baxendale and M. Baumann, *Org. Lett.*, 2010, **12**, 3618; (k) A. B. Leduc and T. F. Jamison, *Org. Process Res. Dev.*, 2012, **16**, 1082.
- (a) A. K. Khatana, V. Singh, M. K. Gupta and B. Tiwari, *Synthesis*, 2018, **50**, 4290; (b) P.-F. Dai, J.-P. Qu and Y.-B. Kang, *Org. Lett.*, 2019, **21**, 1393; (c) K. Takamatsu, M. Kasai, H. Nishizawa, R. Suzuki and H. Konno, *Tetrahedron Lett.*, 2021, **81**, 153320; (d) B. S. Nagy, C. O. Kappe and S. B. Ötvös, *Adv. Synth. Catal.*, 2022, **364**, 1998.
- (a) D. R. Larkin, *J. Org. Chem.*, 1990, **55**, 1563; (b) M. Liu, H. Wang, H. Zeng and C.-J. Li, *Sci. Adv.*, 2015, **1**, e1500020; (c) M. Liu and C. J. Li, *Angew. Chem. Int. Ed.*, 2016, **55**, 10806; (d) H. Yu, S. Ru, G. Dai, Y. Zhai, H. Lin, S. Han and Y. Wei, *Angew. Chem. Int. Ed.*, 2017, **56**, 3867; (e) X. Yan, Y.-H. Lai and R. N. Zare, *Chem. Sci.*, 2018, **9**, 5207; (f) L. J. Durndell, C. Cucuzzella, C. M. Parlett, M. A. Isaacs, K. Wilson and A. F. Lee, *Catal. Today*, 2019, **333**, 161.
- Y. Zhang, Y. Cheng, H. Cai, S. He, Q. Shan, H. Zhao, Y. Chen and B. Wang, *Green Chem.*, 2017, **19**, 5708.
- K.-J. Liu, Y.-L. Fu, L.-Y. Xie, C. Wu, W.-B. He, S. Peng, Z. Wang, W.-H. Bao, Z. Cao and X. Xu, *ACS Sustain. Chem. Eng.*, 2018, **6**, 4916.
- (a) H. L. Bäckström, *J. Am. Chem. Soc.*, 1927, **49**, 1460; (b) H. L. Bäckström and Ü. Riiner, *Acta Chem. Scand.*, 1966, **20**, 630; (c) R. Cundall and A. Davies, *Trans. Faraday Soc.*, 1966, **62**, 2444; (d) I. V. Khudyakov, P. F. McGarry and N. J. Turro, *J. Phys. Chem.*, 1993, **97**, 13234; (e) M. A. Theodoropoulou, N. F. Nikitas and C. G. Kokotos, *Beilstein J. Org. Chem.*, 2020, **16**, 833.
- (a) W. Jorissen and P. van der Beek, *Recl. Trav. Chim. Pays-Bas*, 1926, **45**, 245; (b) P. Van der Beek, *Recl. Trav. Chim. Pays-Bas*, 1932, **51**, 411; (c) T. W. Findley, D. Swern and J. T. Scanlan, *J.*

- Am. Chem. Soc.*, 1945, **67**, 412; (d) C. R. Dick and R. F. Hanna, *J. Org. Chem.*, 1964, **29**, 1218.
- 13 (a) S.-I. Hirashima and A. Itoh, *Chem. Pharm. Bull.*, 2007, **55**, 156; (b) M. Hajimohammadi, N. Safari, H. Mofakham and A. Shaabani, *Tetrahedron Lett.*, 2010, **51**, 4061; (c) N. Iqbal, S. Choi, Y. You and E. J. Cho, *Tetrahedron Lett.*, 2013, **54**, 6222; (d) Z. E. Hamami, L. Vanoye, P. Fongarland, C. de Bellefon and A. Favre-Régouillon, *J. Flow Chem.*, 2016, **6**, 206; (e) J. Xu, X. Yue, L. He, J. Shen, Y. Ouyang, C. Liang and W. Li, *ACS Sustain. Chem. Eng.*, 2022, **10**, 14119; (f) H. Shi, J. Li, T. Wang, M. Rudolph and A. S. K. Hashmi, *Green Chem.*, 2022, **24**, 5835; (g) C. S. Batsika, C. Koutsilieris, G. S. Koutoulogenis, M. G. Kokotou, C. G. Kokotos and G. Kokotos, *Green Chem.*, 2022, **24**, 6224.
- 14 L. Vanoye, M. Abdelaal, K. Grundhauser, B. Guicheret, P. Fongarland, C. De Bellefon and A. Favre-Régouillon, *Org. Lett.*, 2019, **21**, 10134.
- 15 Y. Ogata and Y. Sawaki, *J. Am. Chem. Soc.*, 1972, **94**, 4189.
- 16 J. Yang, J. Jiang, J. Jiang, X. Pan, Y. Pan and L. Ni, *J. Therm. Anal. Calorim.*, 2019, **135**, 2309.
- 17 (a) C. Lehtinen, V. Nevalainen and G. Brunow, *Tetrahedron*, 2001, **57**, 4741; (b) Z. Wang, Y. Qin, H. Huang, G. Li, Y. Xu, P. Jin, B. Peng and Y. Zhao, *Front. Chem.*, 2022, **10**, 855843.
- 18 D. Prat, A. Wells, J. Hayler, H. Sneddon, C. R. McElroy, S. Abou-Shehada and P. J. Dunn, *Green Chem.*, 2016, **18**, 288.
- 19 S. Kato and F. Mashio, *J. Soc. Chem. Ind., Japan.*, 1957, **60**, 1515.
- 20 (a) A. Baeyer and V. Villiger, *Ber. Dtsch. Chem. Ges.*, 1899, **32**, 3625; (b) M. Renz and B. Meunier, *Eur. J. Org. Chem.*, 1999, **1999**, 737.
- 21 L. Vanoye and A. Favre-Régouillon, *React. Chem. Eng.*, 2023, **8**, 1043.
- 22 (a) L. Vanoye, A. Favre-Régouillon, A. Aloui, R. Philippe and C. de Bellefon, *RSC Adv.*, 2013, **3**, 18931; (b) L. Vanoye and A. Favre-Régouillon, *Org. Process Res. Dev.*, 2022, **26**, 335.
- 23 D. Rusinska-Roszak, *Molecules*, 2017, **22**, 481.
- 24 (a) A. Favre-Régouillon, *ACS Sustain. Chem. Eng.*, 2023, **11**, 1619; (b) A. Favre-Régouillon and L. Vanoye, *Green Chem.*, 2023, **25**, 5756; (c) J. Xu, X. Yue, L. He, J. Shen, Y. Ouyang, C. Liang and W. Li, *ACS Sustain. Chem. Eng.*, 2023, **11**, 1622.